

Generation of multi-wavelength square pulses in the dissipative soliton resonance regime by a Yb-doped fiber laser

Xude Wang(汪徐德), Simin Yang(杨思敏), Mengqiu Sun(孙梦秋), Xu Geng(耿旭), Jieyu Pan(潘婕妤),Shuguang Miao(苗曙光), and Suwen Li(李素文)

Citation: Chin. Phys. B, 2021, 30 (**6**): 064212. DOI: 10.1088/1674-1056/abd6f4
Journal homepage: http://cpb.iphy.ac.cn; http://iopscience.iop.org/cpb

What follows is a list of articles you may be interested in

Generation of cavity-birefringence-dependent multi-wavelength bright-dark pulse pair in a figure-eight thulium-doped fiber laser

Xiao-Fa Wang(王小发), Dong-Xin Liu(刘东鑫), Hui-Hui Han(韩慧慧), and Hong-Yang Mao(毛红炀)
Chin. Phys. B, 2021, 30 (**5**): 054205. DOI: 10.1088/1674-1056/abd68f

Zinc-oxide/PDMS-clad tapered fiber saturable absorber for passively mode-locked erbium-doped fiber laser

F D Muhammad, S A S Husin, E K Ng, K Y Lau, C A C Abdullah, and M A Mahdi
Chin. Phys. B, 2021, 30 (**5**): 054204. DOI: 10.1088/1674-1056/abd76e

Suppression of multi-pulse formation in all-polarization-maintaining figure-9 erbium-doped fiber mode-locked laser

Jun-Kai Shi(石俊凯), Deng-Feng Dong(董登峰), Ying-Ling Pan(潘映伶), Guan-Nan Li(李冠楠), Yao Li(黎尧), Li-Tuo Liu(刘立拓), Xiao-Mei Chen(陈晓梅), and Wei-Hu Zhou(周维虎)
Chin. Phys. B, 2021, 30 (**1**): 014206. DOI: 10.1088/1674-1056/abc153

Visible-light all-fiber vortex lasers based on mode selective couplers

Chuchu Dong(董楚楚), Jinhai Zou(邹金海), Hongjian Wang(王鸿健), Han Yao(尧涵), Xianglong Zeng(曾祥龙), Yikun Bu(卜轶坤), Zhengqian Luo(罗正钱)
Chin. Phys. B, 2020, 29 (**9**): 094204. DOI: 10.1088/1674-1056/aba278

Two-dimensionally controllable DSR generation from dumbbell-shaped mode-locked all-fiber laser

Zhi-Yuan Dou(窦志远), Bin Zhang(张斌), Jun-Hao Cai(蔡君豪), Jing Hou(侯静)
Chin. Phys. B, 2020, 29 (**9**): 094201. DOI: 10.1088/1674-1056/ab9de1

Generation of multi-wavelength square pulses in the dissipative soliton resonance regime by a Yb-doped fiber laser*

Xude Wang(汪徐德)[1,†], Simin Yang(杨思敏)[1], Mengqiu Sun(孙梦秋)[1], Xu Geng(耿旭)[1], Jieyu Pan (潘婕妤)[1], Shuguang Miao(苗曙光)[1], and Suwen Li(李素文)[1,2]

[1] School of Physics and Electronic Information, Huaibei Normal University, Huaibei 235000, China
[2] Anhui Province Key Laboratory of Pollutant Sensitive Materials and Environmental Remediation, Huaibei Normal University, Huaibei 235000, China

(Received 13 November 2020; revised manuscript received 17 December 2020; accepted manuscript online 28 December 2020)

Multi-wavelength square pulses are generated in the dissipative soliton resonance (DSR) regime by a Yb-doped fiber laser (YDFL) with a long cavity configuration. The spectral filter effect provided by a passive fiber with low-stress birefringence facilitates the establishment of multi-wavelength operation. Through appropriate control of the cavity parameters, a multi-wavelength DSR pulse can be generated in single- and dual-waveband regions. When the multi-wavelength DSR works in the 1038 nm waveband, the pulse duration can broaden from 2 ns to 37.7 ns. The maximum intra-cavity pulse energy is 152.7 nJ. When the DSR works in the 1038 nm and 1080 nm wavebands, the pulse duration can be tuned from 2.3 ns to 10.5 ns with rising pump power. The emergence of the 1080 nm waveband is attributed to the stimulated Raman scattering (SRS) effect. Our work might help a deeper insight to be gained into DSR pulses in all-normal-dispersion YDFLs.

Keywords: fiber laser, dissipative soliton resonance, square pulse

PACS: 42.55.Wd, 42.81.Dp, 42.60.Fc **DOI:** 10.1088/1674-1056/abd6f4

1. Introduction

Yb-doped fiber lasers (YDFLs), as an excellent type of laser source for generating ultra-short pulses, have considerable potential for use in many scientific and industrial applications, such as bio-medicine, metrology, material processing, and telecommunications.[1,2] Due to the wide gain bandwidth and high gain of Yb-doped fiber, YDFLs are expected to be promising candidates for obtaining high-energy ultrashort pulses, which are more favorable for some practical applications. As opposed to conventional solitons formed by anomalous-dispersion fiber lasers, YDFLs operate in the all-normal dispersion regime, which can produce highly chirped dissipative solitons with energies of up to tens of nJ.[3] However, due to the pulse splitting that occurs in the fiber laser, the production of high-energy pulses by a laser oscillator is a challenge that still remains to be solved.

Depending on the different pulse-shaping mechanisms and dynamics of fiber lasers, various temporally tailored pulses such as Gaussian pulses, step-like pulses, and square pulses have been formed by fiber lasers,[4–9] which can satisfy some demands in various application fields. Among these, square pulses have attracted considerable interest due to their ability to scale the pulse energy.[10] By means of the peak power-clamping effect, square pulses can achieve high pulse energies by broadening their pulse widths with the rising pump power. In particular, dissipative soliton resonance (DSR) is an efficient way to generate high-energy square pulses. As a new kind of soliton, DSR was first theoretically investigated by Chang *et al.* in 2008.[11] In principle, DSR, as a single pulse, can increase the pulse width indefinitely while keeping its amplitude fixed, which consequently results in the generation of a pulse with infinite energy.[12,13] It has been demonstrated that using the appropriate cavity parameters, DSRs can be formed in various types of fiber laser,[14–20] regardless of mode-locking mechanisms and cavity dispersion regimes, even in all-normal dispersion YDFLs. Indeed, Wang *et al.* investigated unusual DSR pulse evolution in a YDFL mode locked by a nonlinear fiber loop mirror.[21] Yu *et al.* reported a high-energy DSR pulse in a YDFL using a nonlinear polarization rotation (NPR) technique.[22] The maximum output pulse energy was able to reach 34 nJ. Li *et al.* demonstrated the generation of an ultra-wide DSR pulse in a YDFL, which was achieved by the NPR technique.[23] The pulse width was able to be tuned from 58.6 ns to 431 ns. Nevertheless, most DSR pulse research has mainly focused on single-wavelength operation. In some applications, fiber lasers that generate multi-wavelength pulses would be more advantageous. Therefore, multi-wavelength DSRs delivering at wavelengths of around 1 μm need to be further investigated.

It is well known that a lower repetition rate in a long ring cavity implies a higher pulse energy for a given average output power. In this paper, we report on the generation of

*Project supported by the National Natural Science Foundation of China (Grant No. 41875040), the Natural Science Foundation of Anhui Province, China (Grant No. 2008085MF211), the Foundation for Young Talents in College of Anhui Province (Grant No. gxyqZD2019034), and the Key Natural Science Research Project for Colleges and Universities of Anhui Province, China (Grant No. KJ2020A0027).

†Corresponding author. E-mail: wangxude@chnu.edu.cn

© 2021 Chinese Physical Society and IOP Publishing Ltd

multi-wavelength square pulses in the DSR regime in a passively mode-locked YDFL with a long cavity configuration. A 300-m single mode fiber (SMF, HI-1060) is inserted into a resonator to prolong the cavity length, so that the total cavity length reaches 311.3 m, corresponding to the low fundamental frequency of 661.6 kHz. Multi-wavelength operation is realized by an artificial comb filter, and is caused by stress birefringence of the fiber. The wavelength spacing is 1.8 nm. When the multi-wavelength DSR works in the 1038 nm waveband, the pulse width broadens linearly from 2 ns to 37.7 ns without wave breaking. The maximum output single-pulse energy is 15.27 nJ through a 10% fiber coupler. Moreover, by appropriately changing the cavity parameters, the multi-wavelength DSR pulse can also operate in dual wavebands, which are located at 1038 nm and 1080 nm, respectively. By increasing the pump power, the duration of the DSR can be tuned from 2.3 ns to 10.5 ns, and the pulse energy increased from 3 nJ to 9.7 nJ. Our work might help deeper insight to be gained into DSR pulses in all-normal-dispersion YDFLs.

2. Experimental setup

For the proposed YDFL, we implemented a ring cavity, as illustrated in Fig. 1. The gain section was a 62 cm YDF (Nufern, SM-YSF-HI), which was excited by a 976 nm pump source with a maximum launched power of 500 mW. The mode-locking operation was accomplished based on the NPR mechanism, comprising a polarization-dependent isolator (PD-ISO) and two polarization controllers (PCs). Meanwhile, two PCs were used to optimize the mode locking by adjusting the light polarization state, and a PD-ISO was employed to ensure the mono-directional transmission of the laser. In order to prolong the length of the cavity and lower the repetition rate, a piece of SMF 300 m long was spliced into the cavity. The whole cavity length was 311.3 m, corresponding to a fundamental frequency of 661.6 kHz. Approximately 10% of the laser output was extracted via a fiber coupler for analysis. An oscilloscope and an optical spectrum analyzer were utilized to measure the temporal and spectral properties of the output pulses. The operational stability was monitored by a radio-frequency (RF) spectrum analyzer.

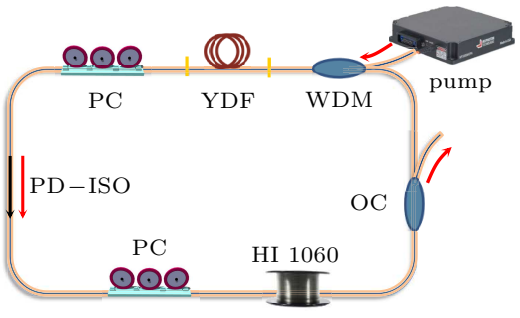


Fig. 1. Experimental schematic of a YDFL with a long cavity configuration.

3. Results and analysis

Mode locking can be achieved at a forward pump power of 110 mW. With fine adjustment of the PCs, a low-repetition-rate square pulse with a nanosecond width is observed from 150 mW to 500 mW. The characteristics of the typical square pulse at 350 mW are depicted in Fig. 2.

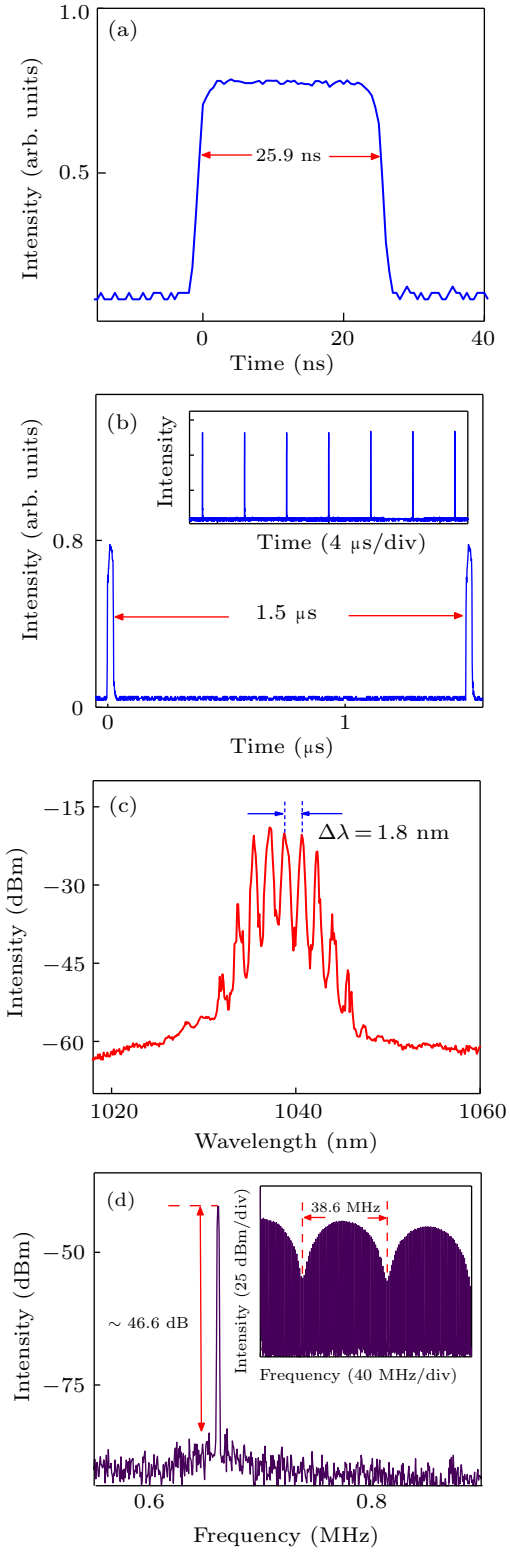


Fig. 2. Generation of a square pulse at 1038 nm. (a) Square pulse; (b) pulse train; (c) spectrum; (d) RF spectrum (inset: RF spectrum over a 100 MHz span).

Figure 2(a) shows a single mode-locked pulse. A single pulse from the fiber laser exhibits a rectangular shape. The edge-to-edge width of the square pulse is ∼ 25.9 ns. Figure 2(b) presents the pulse train. The interval is 1.5 μs, corresponding to the cavity roundtrip time. We can see that each pulse appears as a square shape with equal amplitude. The spectrum is shown in Fig. 2(c), which is different from the spectra of YDFLs reported before. The spectrum exhibits multi-wavelength lasing with a wavelength spacing of 1.8 nm and the central position of the waveband is 1038 nm. The multi-wavelength lasing in the experiment can be explained as the effect of filtering induced by fiber birefringence. In the experiment, we tried to measure the autocorrelation trace of this square pulse. However, no coherent peak was observed in the autocorrelation trace, indicating that this square pulse is a single DSR but not a bunch of pulses.[24] The fundamental frequency is measured by an RF analyzer, as shown in Fig. 2(d). The peak of the RF spectrum is located at 661.6 kHz with a signal-to-noise ratio (SNR) of ∼ 46.6 dB, which matches the 311.3-m cavity length. Moreover, the RF spectrum over a span of 100 MHz is shown in the inset of Fig. 2(d). Here, it can clearly be seen that the envelope of the RF spectrum is periodically varied, and that the modulation period is 38.6 MHz, corresponding to a pulse width of ∼ 25.9 ns in the temporal domain. Note that routine dissipative solitons without multi-wavelength lasing are also observed in the experiment when the PCs are properly adjusted. However, the dissipative soliton does not operate in the DSR regime.

To further verify that this square pulse is due to DSR, we fixed the PCs and gradually increased the pump power to characterize the pulse evolution features. The temporal and spectral evolutions are presented in Fig. 3. While the pump power is rising, the pulse keeps its square profile without shape distortion and the pulse amplitude remains constant, as presented in Fig. 3(a). The pulse duration broadens linearly with the pump power. The corresponding spectra at different pump powers are shown in Figs. 3(b) and 3(c). As the pump power increases, the emission spectrum bandwidth is gradually broadened, while the position of the central wavelength remains almost invariant (at ∼ 1038 nm). The number of multi-wavelength lasing peaks increases with the pump power, while the spacing is fixed at 1.8 nm for all pump powers. To better clarify the characteristics of the square pulse, the relationships between the pulse width and pulse energy with respect to the input pump powers are shown in Fig. 3(c). When the pump power is increased from 150 mW to 500 mW, the pulse width linearly widens from 2 ns to 37.7 ns. Similarly, the single-pulse energy increases from 3 nJ to 15.27 nJ. Therefore, the evolutionary trend of the square pulse is in accordance with DSR theory.[25] The maximum output power is 10.1 mW, corresponding to a pulse energy of 15.27 nJ. Considering that 10% of the pulse energy is taken from the cavity, the intra-cavity pulse energy is around 152.7 nJ. It should be noted that the maximum pulse energy and pulse width in our experiment are primarily limited by the pumped power. Thus, we think that the pulse energy and width might be further increased if a higher-power pump source were to be used.

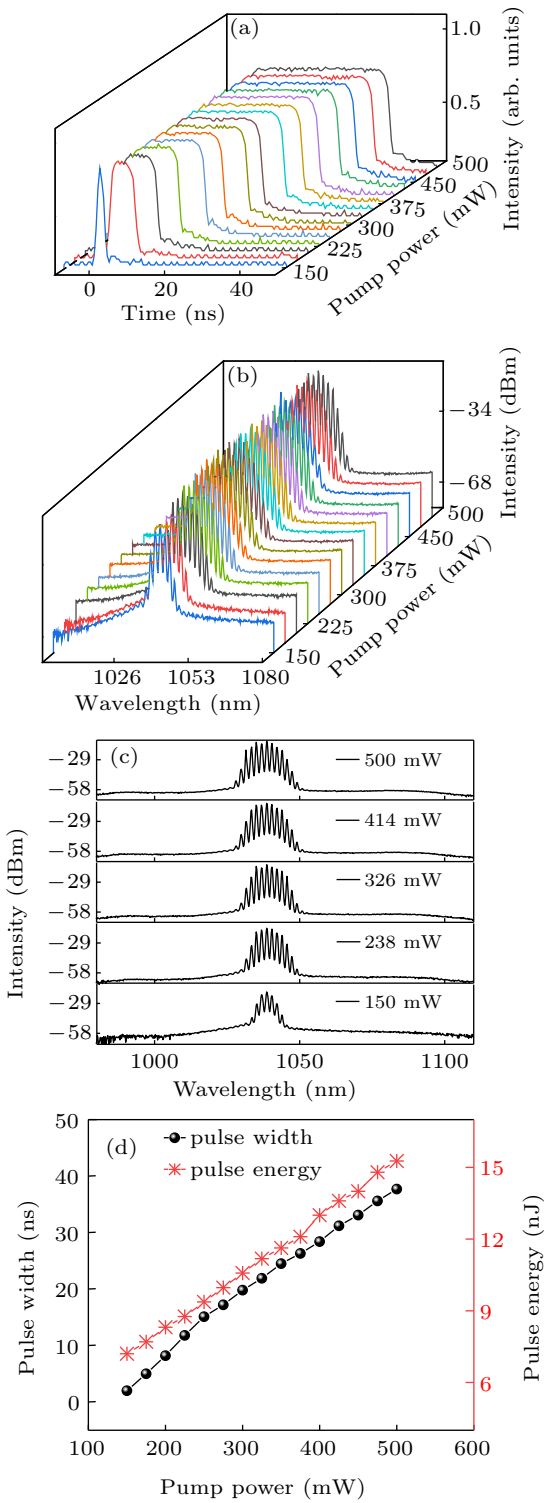


Fig. 3. Evolution of the properties of the square pulse at 1038 nm. (a) Pulse evolution versus pump power. (b) Corresponding spectral evolution. (c) Comparison of the spectra under different pump powers. (d) Pulse width and energy versus pump power.

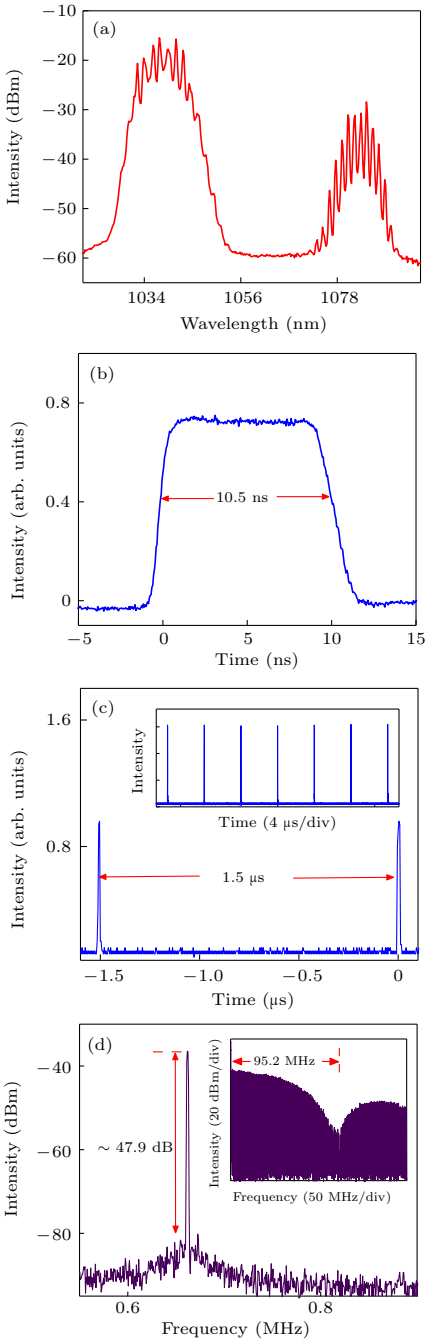


Fig. 4. Generation of square pulses at 1038 nm and 1080 nm. (a) Spectrum; (b) square pulse; (c) pulse train; (d) RF spectrum (inset: RF spectrum over a span of 150 MHz).

By rotating the PCs and changing the pump power, another type of square pulse with a different spectral structure is formed in the fiber laser. Compared to the multi-wavelength spectrum in the 1038 nm waveband region, here, the changes in spectrum are evident, as shown in Fig. 4(a). Figure 4(a) shows the typical spectrum of the multi-wavelength lasing operated in the 1038 nm and 1080 nm wavebands at a pump power of 500 mW. The spectral component in the waveband at approximately 1080 nm gradually emerges with an increase in pump power. The spacing between the two wavebands is $\sim$ 40 nm, thus, the generation of the secondary waveband is due to the stimulated Raman scattering (SRS) effect.[26] A quasi-square pulse with a flat-topped shape and a pulse width of 10.5 ns is generated, as shown in Fig. 4(b). It should be noted that the trailing edge of the pulse is not as steep, which might be affected by the SRS. Figure 4(c) presents a stable pulse train with a pulse-to-pulse interval of 1.5 μs. The typical RF spectrum shown in Fig. 4(d) has a SNR of around 47.9 dB at 661.6 kHz. The RF spectrum over a span of 150 MHz in the inset exhibits a modulation frequency of 95.2 MHz, corresponding to a pulse duration of 10.5 ns.

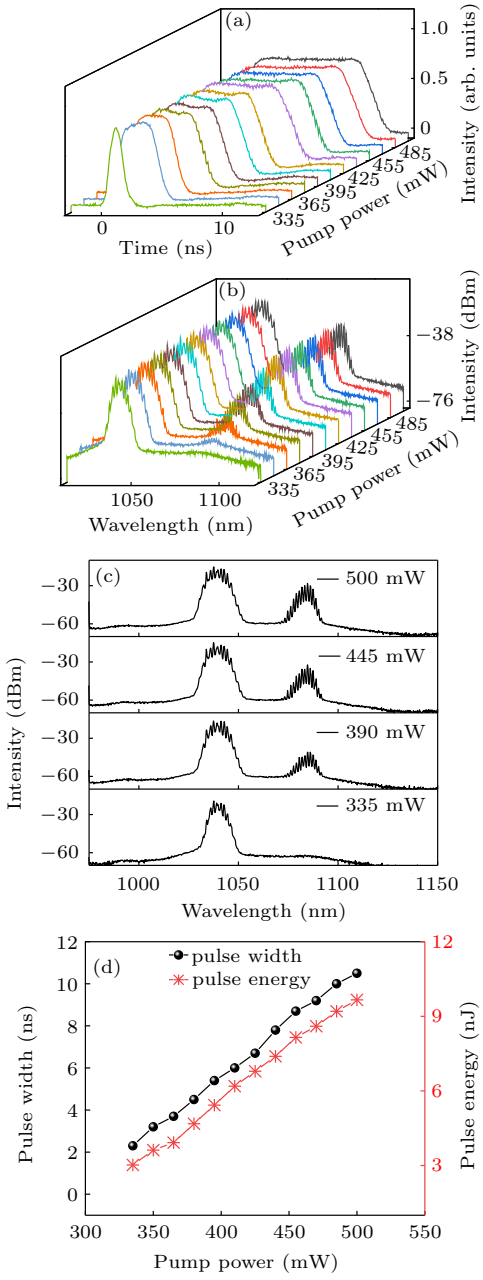


Fig. 5. Evolution of the properties of a square pulse operating in dual wavebands. (a) Pulse evolution versus pump power. (b) Corresponding spectral evolution. (c) Comparison of the spectra under different pump powers. (d) Pulse width and energy versus pump power.

In order to further verify the influence of pump power on this DSR pulse, we record the evolution of the characteristics of the pulses under different pump powers. The temporal evolution is shown in Fig. 5(a). Under dual-waveband operation,

the DSR pulse can still broaden with the pump power, while the pulse amplitudes remain almost invariable. The spectral evolution is shown in Figs. 5(b) and 5(c). Multi-wavelength lasing emerges simultaneously in the 1038 nm and 1080 nm wavebands. An increase in the pump power causes clear enhancement of the SRS components at 1080 nm. Figure 5(d) clearly shows the relationship between the pulse width and the output single-pulse energy as a function of the pump power. When the pump power is increased from 335 mW to 500 mW, the square pulses are broadened from 2.3 ns to 10.5 ns, and the single-pulse energy increases from 3 nJ to 9.67 nJ. These results are inconsistent with DSR theory. Compared with a DSR in the 1038 nm waveband, the square DSR pulse in dual-waveband operation has a narrower pulse duration and a lower pulse energy for the same pump power. This is partly because the cavity parameters are influenced by the orientation of PCs, and partly because the advent of SRS takes part of the pump energy. Thus, SRS imposes a limitation on the energy scalability of DSR in this experiment. It has been reported that SRS can cause DSR pulse instability.[21] However, the pulse still remains stable at the maximum pump power of 500 mW in our experiment. According to experimental observation, the fiber laser could sustain DSR operation for a long time if there were no environmental perturbations applied to the fiber laser.

In previous literature, DSR operation under multi-wavelength mode locking has rarely been reported. In our experiment, multi-wavelength square pulses are frequently observed in the fiber laser without the insertion of any external filter devices such as comb filters and polarization-maintaining fibers (PMFs). We attribute this to the birefringence-induced filtering effect. As we know, the NPR structure is composed of two PCs and a PD-ISO. By rotating the PCs, an artificial birefringence-induced spectral filter effect may be formed, originating from the weak intra-cavity birefringence of the passive fiber.[27] Therefore, NPR has a double role: it plays a role in mode-locking and a role in achieving multi-wavelength lasing. In order to confirm that multi-wavelength operation is caused by stress birefringence, we also measured the output spectra of multi-wavelength continuous-wave (CW) lasing by adjusting the pump powers. As can be seen in Fig. 6, the wavelength spacing between adjacent CW lasing peaks is ~ 1.8 nm, which is consistent with that in mode-locked lasing. The lasing peaks are located in the 1038 nm waveband, and the number of multi-wavelength peaks increases with the pump power. In addition, we use a self-consistent calculation to verify that the wavelength spacing is introduced by the stress birefringence due to the passive fiber. The wavelength spacing can be described by the formula $\lambda = \lambda^2/(BL)$, where λ denotes the central wavelength, L is the cavity length and B is the strength of the SMF.[28] Accord to the experimental results, we are able to determine that $\lambda = 1.8$ nm, $L = 311.3$ m, and $\lambda = 1038$ nm. Thus, the birefringence should be 0.2×10^{-5}, which is very close to the birefringence of the SMF. Therefore, the experimental and computational results show that the passive fiber with low stress birefringence is responsible for multi-wavelength lasing in this experiment.

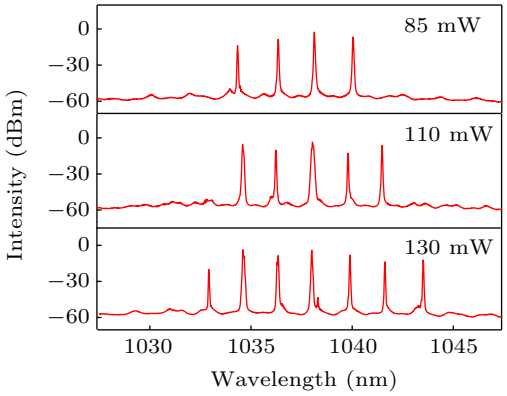


Fig. 6. Multiwavelength lasing at different pump powers.

4. Conclusions

In summary, multi-wavelength DSR pulses have been experimentally achieved in an all-normal-dispersion YDFL with a long cavity. Benefiting from the spectral filter effect induced by the low stress birefringence of the passive fiber in the NPR-based fiber laser, mode-locked and multi-wavelength lasing were achieved simultaneously. By adjusting the pump power and PCs, the multi-wavelength DSR can operate in different wavebands. When the DSR works in the region of the 1038 nm waveband, the pulse duration can broaden from 2 ns to 37.7 ns. The maximum output pulse energy is 15.27 nJ at 500 mW. When the multi-wavelength DSR works in the 1038 nm and 1080 nm wavebands, the pulse duration can be tuned from 2.3 ns to 10.5 ns and the pulse energy can be increased from 3 nJ to 9.7 nJ. The emergence of the 1080 nm waveband is attributed to the SRS effect. Our work might help a deeper insight to be gained into the nonlinear dynamics of square-wave pulses in all-normal-dispersion YDFLs.

References

[1] Fermann M E and Hartl I 2013 *Nat. Photon.* **7** 868
[2] Schibli T R, Hartl I, Yost D C, Martin M J, Marcinkevičius A, Fermann M E and Ye J 2008 *Nat. Photon.* **2** 355
[3] Kharenko D S, Podivilov E V, Apolonski A A and Babin S A 2012 *Opt. Lett.* **37** 4104
[4] Peng J S, Zhan L, Gu Z C, Qian K, Luo S Y and Shen Q S 2012 *Opt. Commun.* **285** 731
[5] Mao D, Liu X M, Wang L R, Lu H and Duan L N 2011 *Opt. Express* **19** 3996
[6] Li X L, Zhang S M, Zhang H X, Han M M, Wen F and Yang Z J 2014 *IEEE Photon. Technol. Lett.* **26** 2082
[7] Semaan G, Braham F B, Salhi M, Meng Y C, Bahloul F and Sanchez F 2016 *Opt. Express* **24** 8399
[8] Wu T Y, Dou Z Y, Zhang B and Hou J 2020 *Chin. Phys. B* **29** 014202
[9] Duan L N, Wen J, Fan W and Wang W 2017 *Chin. Phys. B* **26** 104205
[10] Zhang X M, Gu C, Chen G L, Sun B, Xu L X, Wang A T and Ming H 2012 *Opt. Lett.* **37** 1334
[11] Chang W, Ankiewicz A, Soto-Crespo J M and Akhmediev N 2008 *Phys. Rev. A* **78** 023830

[12] Wu X, Tang D Y, Zhang H and Zhao L M 2009 *Opt. Express* **17** 5580
[13] Deng Z S, Zhao G K, Yuan J Q, Lin J P, Chen H J, Liu H Z, Luo A P, Cui H, Luo Z C and Xu W C 2017 *Opt. Lett.* **42** 4517
[14] Zhao K J, Wang P, Ding Y H, Yao S Y, Gui L L, Xiao X S and Yang C X 2019 *Appl. Phys. Express* **12** 012002
[15] Semaan G, Braham F B, Fourmont J, Salhi M, Bahloul F and Sanchez F 2016 *Opt. Lett.* **41** 4767
[16] Mei L, Chen G L, Xu L X, Zhang X M, Gu C, Sun B and Wang A T 2014 *Opt. Lett.* **39** 3235
[17] Zhao N, Liu M, Liu H, Zheng X W, Ning Q Y, Luo A P, Luo Z C and Xu W C 2014 *Opt. Express* **22** 10906
[18] Wang H, Du T J, Li Y H, Zou J H, Wang K J, Zheng F Y, Fu J F, Yang J H, Fu HY and Luo Z Q 2019 *Chin. Opt. Lett.* **17** 030602
[19] Wang Z K and Wu W D 2021 *Opt. Laser Technol.* **133** 106503
[20] Lyu Y J, Shi H X, Wei C, Li H P, Li J F and Liu Y 2017 *Photon. Res.* **5** 612
[21] Wang Y F, Li L, Zhao J Q, Wang S, Shu C J, Su L, Tang D Y, Shen D Y and Zhao L M 2019 *IEEE Photon. J.* **11** 1500509
[22] Yu H L, Wang X L, Zhou P, Xu X J and Chen J B 2015 *IEEE Photon. Technol. Lett.* **27** 737
[23] Cao Y F, Jia D F, Liu T H, Yang T X, Wang Z Y and Ge C F 2017 *Appl. Opt.* **56** 6742
[24] Semaan G, Niang A, Salhi M and Sanchez F 2017 *Laser Phys. Lett.* **14** 055401
[25] Grelu P, Chang W, Ankiewicz A, Soto-Crespo J M and Akhmediev N 2010 *J. Opt. Soc. Am. B* **27** 2336
[26] Runge A F J, Aguergaray C, Broderick N G R and Erkintalo M 2014 *Opt. Lett.* **39** 319
[27] Jin X X, Wang X, Wang X L and Zhou P 2015 *Appl. Opt.* **54** 8260
[28] Huang S S, Wang Y G, Yan P G, Zhao J Q, Li H Q and Lin R Y 2014 *Opt. Express* **22** 11417